Persistent Molecular Superfluid Response in Doped Para-Hydrogen Clusters

P. L. Raston,[1] W. Jäger,[1,*] H. Li,[2,3] R. J. Le Roy,[2] and P.-N. Roy[2,†]

[1]*Department of Chemistry, University of Alberta, Edmonton, Alberta T6G 2G2, Canada*
[2]*Department of Chemistry, University of Waterloo, Waterloo, Ontario N2L 3G1, Canada*
[3]*Institute of Theoretical Chemistry, State Key Laboratory of Theoretical and Computational Chemistry, Jilin University, 2519 Jiefang Road, Changchun 130023, People's Republic of China*

(Received 31 July 2011; published 19 June 2012)

Direct observation of superfluid response in *para*-hydrogen (p-H_2) remains a challenge because of the need for a probe that would not induce localization and a resultant reduction in superfluid fraction. Earlier work [H. Li, R. J. Le Roy, P.-N. Roy, and A. R. W. McKellar, Phys. Rev. Lett. **105**, 133401 (2010)] has shown that carbon dioxide can probe the effective inertia of p-H_2 although larger clusters show a lower superfluid response due to localization. It is shown here that the lighter carbon monoxide probe molecule allows one to measure the effective inertia of p-H_2 clusters while maintaining a maximum superfluid response with respect to dopant rotation. Microwave spectroscopy and a theoretical analysis based on Feynman path-integral simulations are used to support this conclusion.

DOI: 10.1103/PhysRevLett.108.253402 PACS numbers: 36.40.Ei, 36.40.Mr, 67.25.dw

Apart from helium, para-hydrogen (p-H_2) is the only substance that is expected to exhibit superfluid behavior under laboratory conditions [1]. While bulk p-H_2 freezes at 14 K, nanoclusters remain liquidlike [2] down to at least the estimated superfluid transition temperature of 1.1 K [3]. Direct observation of superfluidity in small p-H_2 clusters has remained a challenge, however, because of the need for a probe that would not induce localization and a concomitant reduction of the superfluid fraction. Initial efforts have shown that carbon dioxide can probe the effective inertia of p-H_2 clusters although larger clusters exhibit a depressed superfluid response due to the strong interactions with the guest molecule [4]. Here we show that the lighter carbon monoxide molecule allows one to probe the superfluid response of p-H_2 clusters while maintaining a maximum superfluid fraction. In a broader sense, using a lighter probe can be viewed as a way to tune the quantumness of the response properties. Such concepts have recently been used to explain dynamical reentrance phenomena in glassy quantum systems [5].

To probe quantum clusters such as $(p\text{-}H_2)_N$ and He_N spectroscopically, it is convenient to dope them with a single chromophore molecule. Microwave and infrared studies of He_N-molecule clusters have revealed that signatures of superfluidity become apparent at relatively low numbers (N) of solvating helium atoms, such as $N = 10$ in the case of He_N-OCS [6,7]. Nonclassical increases in the values of the rotational constants B (inversely proportional to the cluster moment of inertia) were found at and above these critical cluster sizes. This implies a significant decoupling of helium density from the rotational motion of the molecule, and was interpreted to mark the onset of microscopic superfluidity [6], an idea that has been confirmed by simulations [8,9].

Toennies, Vilesov, and co-workers have measured infrared spectra of $(p\text{-}H_2)_N$-OCS clusters embedded within helium nanodroplets [10–12]. Their initial study focused on clusters with $N = 14$–16 p-H_2 molecules, which revealed a disappearance of the Q branch (rovibrational transitions with selection rule $\Delta J = 0$; J is the rotational angular momentum quantum number) upon cooling the droplet from 0.38 K to 0.15 K. This implies that angular momentum is no longer excited about the OCS axis, and it was interpreted that $(p\text{-}H_2)_N$ turns superfluid in the dimension that is parallel to this axis [10]. However, it was later found that the Q branch was also absent for $N = 5$ and 6 and present for $N = 1$–4, 7, and 8 [11], which markedly differs from the bare $(p\text{-}H_2)_N$-OCS clusters for which no Q branch was observed up to at least $N = 7$ [13,14]. This suggests that the spectral anomalies for the $N = 14$–16 clusters may also be related to the helium nanodroplet environment rather than to superfluidity of p-H_2. Several alternative explanations for these anomalies have been proposed [15–17].

The spectroscopic studies of $(p\text{-}H_2)_N$-OCS clusters embedded in helium nanodroplets also showed that the cluster moment of inertia increases steadily up to at least $N = 16$ [11,12]. This indicates that p-H_2 density does not appreciably decouple from the rotation of OCS in this size range. This classical behavior is qualitatively consistent with path-integral Monte Carlo (PIMC) simulations of isolated $(p\text{-}H_2)_N$-OCS clusters which do not predict significant superfluid fractions for N up to and including 17 [(superfluid helium density, ρ_s)/(total helium density, ρ) ≤ 0.2] [18]. In contrast, simulations of small ($N = 3$–25) undoped p-H_2 clusters predict them to be almost entirely superfluid [19–21].

Superfluid response to dopant rotation has recently been confirmed in $(p\text{-}H_2)_N$-CO_2 clusters [4] although the

phenomenon appears to subside as clusters increase in size due to localization caused by relatively strong interactions between CO_2 and p-H_2. The localizing effect of the probe molecule on surrounding p-H_2 molecules depends largely on the strength and anisotropy of the interaction, as well as on the rotational constant of the probe. Carbon monoxide is a better probe molecule for the following reasons: (1) the binding energy of H_2-CO (35 K) is much lower than that of most other possible systems, such as H_2-OCS (110 K), and it is comparable to the chemical potential of small pure p-H_2 clusters ($\approx$ 20–40 K) [22]; (2) the H_2-CO potential energy surface is very weakly anisotropic; and (3) the rotational constant of CO is relatively large. These factors all favor significant delocalization of p-H_2 around CO, a system for which superfluid behavior is expected to occur [23,24]. Additional impetus for the study of $(p\text{-}H_2)_N$-CO clusters comes from the recent report on He_N-CO clusters, where significant decoupling of He_N density from CO rotation was observed at low N [25].

In order to obtain the necessary experimental data for the analysis discussed below, we have reexamined the previously reported infrared spectra of $(p\text{-}H_2)_N$-CO clusters [26] using the results from the microwave spectra reported here. In the infrared study, both a- and b-type $R_1(0)$ transitions ($\nu = 1 \leftarrow 0$, $J = 1 \leftarrow 0$) of clusters with $N \leq 14$ were detected and assigned with the aid of simulations. Separation of the rotational and vibrational contributions to the line positions was, for the most part, not possible. The frequencies of pure rotational transitions in the a-type series, measured in the current study, enabled us to extract from the infrared spectra [26] the vibrational band shift of CO as a function of N, and subsequently the rotational frequencies in the b-type series. We follow the PIMC approach used and described in Refs. [4,27,28]; bosonic exchange is sampled using the worm algorithm [29].

Two sets of predicted a-type rotational frequencies for $(p\text{-}H_2)_N$-CO clusters were available from the infrared study to aid in the search for microwave transitions. The first was obtained from the experimental data under the assumption that the vibrational band shift decreases linearly from $N = 1$ to 7, utilizing the known shift for $(p\text{-}H_2)_1$-CO [30]. Another set of predictions was available from rotational dynamics simulations which employed the reptation quantum Monte Carlo algorithm [26]. Seven lines were found in the frequency range from 10 to 26 GHz which correspond to the a-type $J = 1 - 0$ rotational transitions of $(p\text{-}H_2)_2$-CO through $(p\text{-}H_2)_8$-CO (see Table I).

TABLE I. Measured a-type transition frequencies (in MHz) for $(p\text{-}H_2)_N$-CO clusters.

N	$J = 1 \leftarrow 0$	N	$J = 1 \leftarrow 0$	N	$J = 1 \leftarrow 0$
2	22 200.9333	5	14 633.3349	7	17 723.2247
3	16 455.9571	6	13 243.9010	8	23 867.2029
4	15 107.5316				

The N number assignment relied largely on the transition intensity variations with the p-H_2 concentration in the sample gas mixture. Also used to aid the assignment was a requirement for consistency in the isotopologue data, the trend in the measured transition frequencies in comparison to that obtained from the simulations, the scarcity of other lines, and the smoothness of the vibrational shift. The vibrational band shift of CO is determined by subtracting the microwave transition frequencies from those of the a-type infrared transitions [26], thus assuming that the rotational frequencies are the same in the ground and first-excited vibrational states. The vibrational shift is not smooth, however, unless some of the tentatively identified a-type lines in the infrared study are reassigned; we propose that the original "$N = 7$" line actually corresponds to $N = 6$ and 8, and that the "$N = 6$" line is in fact $N = 7$. The vibrational shift then becomes very smooth and agrees with the calculated values (see Fig. 1). The calculated values are obtained from PIMC using the approach described in Ref. [28] where one averages the difference in interaction potential between the ground and first-excited vibrational state of CO. Note that the experimental results are for transition frequencies between quantum states and therefore independent of temperature. Moreover, the initial state for those transitions is the ground rovibrational state of the complex. This is why we perform our simulations at very low temperature. The PIMC results for 0.25 K and 0.5 K presented in Fig. 1 are nearly identical and agree very well with experiment.

The vibrational shift becomes increasingly nonlinear with larger N, to a much greater magnitude than was the

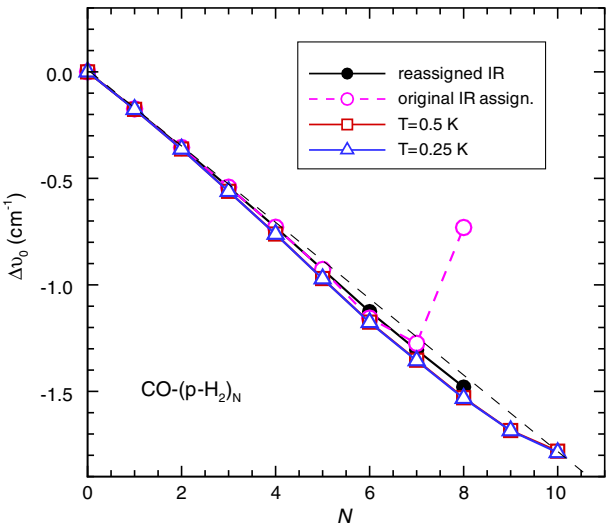

FIG. 1 (color online). Vibrational band shift of $(p\text{-}H_2)_N$-CO clusters with respect to the value for free CO (Ref. [26]). Experimental values for the original (open circles) and switched (solid circles) infrared assignments, and theoretical values at two different temperatures (squares at 0.5 K and triangles at 0.25 K). The dashed line shows an assumed linear shift from $N = 1$ and is for reference only.

case for He_N-CO for the same cluster sizes [25,31]. This is reasonable since the binding energy of H_2-CO is larger than that of He-CO by a factor of 3.5. From the vibrational shift, we then determine the rotational frequencies in the b-type series. We note that these values are approximate, but they should be accurate to within 1% of the actual values by comparison with He_N-CO. The $J = 1 - 0$ frequencies are given by $2B$ in the a-type series and $2b$ in the b-type series, assuming that centrifugal distortion effects may be neglected. Here B and b are the end-over-end (overall complex rotation) and free-molecule rotational constants and are plotted in Fig. 2(a). With increasing N, the a-type series evolves in character from the end-over-end rotation of the complex, and the b-type series evolves from the free-molecule rotation of CO. It is the weak angular anisotropy of the p-H_2-CO interaction coupled with the large rotational constant of CO which allows for the b-type series to occur. This behavior is unlike that for the other $(p\text{-}H_2)_N$ molecule systems studied thus far and requires a modified approach for determining the experimental superfluid fraction, as outlined below.

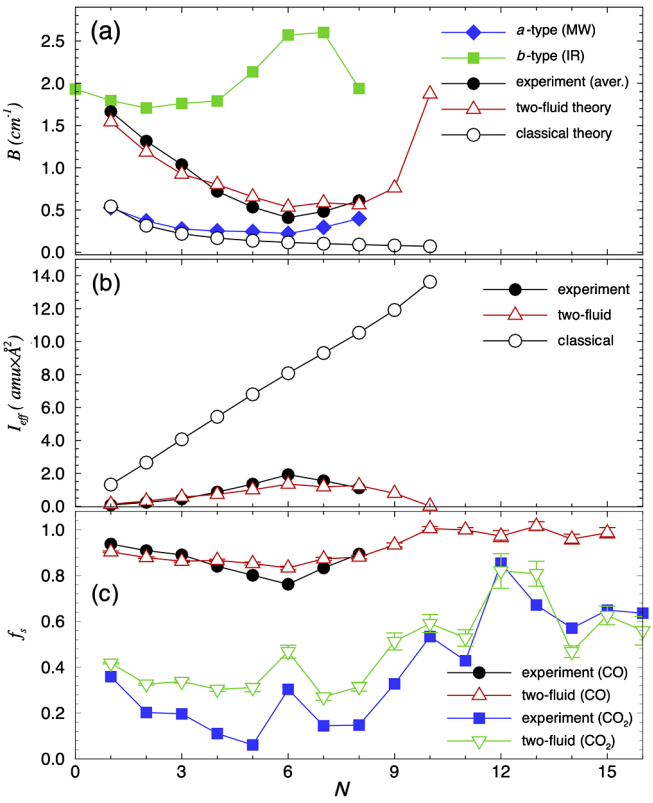

FIG. 2 (color online). (a) Experimental a-type series (diamonds), b-type series (squares), weighted average (filled circles), and theoretical two-fluid (triangles) and classical (open circles) rotational constants for $(p\text{-}H_2)_N$-CO. (b) Experimental (filled circles) and theoretical two-fluid (triangles) and classical (open circles) moments of inertia of $(p\text{-}H_2)_N$. (c) Experimental (circles) and theoretical (triangles) superfluid fraction of p-H_2. Experimental (squares) and theoretical (down triangles) results for $(p\text{-}H_2)_N$-CO_2 from Ref. [4].

We obtain an average effective moment of inertia $I_{\text{eff,cluster}}$ due to both the end-over-end rotation (I_B) and free-molecule rotation (I_b) using second-order perturbation theory. The perturbed Hamiltonian is

$$H = H_0 - \mu_z E_z \cos\alpha \tag{1}$$

where H_0 is the free-cluster Hamiltonian, $\cos\alpha$ is the projection of the cluster axis onto the z-axis of the space-fixed frame, μ_z is the dipole moment magnitude along z, and E_z is the z-component of the electric field strength. The change in ground-state energy due to the field (Stark shift) may be written as

$$\Delta E_0^2 = -\sum_n \frac{|\langle 0|\cos\alpha|n\rangle|^2 \mu_z^2 E_z^2}{E_n - E_0}. \tag{2}$$

For a rigid rotor in the ground state, the change in energy is related to the rotational constant B as $\Delta E_0^{(2)} = -\frac{\mu_z^2 E_z^2}{6B}$ [32]. Since $B = \frac{\hbar^2}{2I}$, the energy change can be written as $\Delta E_0^{(2)} = -\frac{\mu_z^2 E_z^2}{3\hbar^2} I$. This suggests that we can use the second-order Stark shift to determine the effective inertia of doped clusters, and hence their superfluid fraction. Indeed, within this model the effective inertia of the cluster will be $I_{\text{eff,complex}} = -\frac{3\hbar^2}{\mu_z^2 E_z^2}\Delta E_0^{(2)}$, and using Eq. (2) we obtain an expression in terms of transition frequencies and dipole moment matrix elements,

$$I_{\text{eff,complex}} = \sum_n \frac{3|\langle 0|\cos\alpha|n\rangle|^2 \hbar^2}{E_n - E_0}. \tag{3}$$

The two major contributions to the above sum are the end-over-end rotation and free-molecule rotation transition frequencies that appear in the denominator. The dipole matrix elements add up to $1/3$ in a complete basis, and the $3|\langle 0|\cos\alpha|n\rangle|^2$ factors are the normalized spectral weights of Ref. [26]. The above expression also suggests a way to obtain effective rotational constants B_{eff}, which we show in Fig. 2(a). The most interesting aspect is the fact that B_{eff} is much larger than the values predicted by a classical model [open circles in Fig. 2(a)], thus implying significant decoupling of p-H_2 density from the cluster rotation.

For systems undergoing rotation, the superfluid fraction is defined in terms of nonclassical rotational inertia. To define the superfluid fraction, one adopts a two-fluid model where it is assumed that the total density of the fluid is the sum of the contributions from a normal and a superfluid component $\rho_{\text{total}} = \rho_n + \rho_s$. The superfluid fraction is $f_s = \rho_s/\rho_{\text{total}}$ while the normal fraction is $f_n = \rho_n/\rho_{\text{total}}$. The normal fraction is calculated as the ratio of the effective over the classical inertia of hydrogen $f_n = I_{\text{eff}}/I_{\text{classical}}$. We used the area estimator [33] to calculate the superfluid fraction with respect to dopant rotation

within our PIMC simulations. This is different from the space-fixed frame response usually used to study pure hydrogen clusters as in, for instance, Ref. [19]. The rotational constants were calculated under the assumption of this two-fluid model for superfluidity and are shown in Fig. 2(a). These values correspond to the perpendicular response with respect to the dopant axis and are quite high for all cluster sizes. The agreement with the B_{eff} values from the experimental data is excellent and justifies our approach in obtaining the average effective moments of inertia from the experimental data. The corresponding values are related to the normal fraction of hydrogen as predicted by linear response theory. We are in the presence of a ''composite'' superfluid response. Two kinds of excitations are possible and have to be accounted for when analyzing the superfluid response. The intensities (spectral weights) are used to obtain a weighted average inertia. It appears that linear response theory probes the same inertia. The calculated classical- and effective-inertia values are shown in Fig. 2(b). The superfluid fraction is then obtained as $f_s = 1 - f_n$. The superfluid fraction calculated from the PIMC simulations is shown in Fig. 2(c). We now compare the calculated I_{eff} and f_s values to experimental estimates. To obtain the experimental superfluid fraction we use the approach proposed in Ref. [27]. The idea is to use the experimental B_{eff} constants to obtain the total moment of inertia of the system by inverting the relation $B_{\mathrm{eff}} = \hbar^2/(2I_{\mathrm{eff,complex}})$. The effective inertia of the hydrogen environment is then obtained by subtracting the inertia of the CO molecule from the total inertia of the complex, $I_{\mathrm{eff}} = I_{\mathrm{eff,complex}} - I_{\mathrm{CO}}$. The results are shown in Fig. 2(b) where they are seen to agree excellently with theoretical predictions and to differ greatly from the monotonically increasing classical values; this is a clear sign of a pronounced decoupling between the dopant rotation and the hydrogen environment. Results for the experimental superfluid fraction are shown in Fig 2(c). The superfluid fractions, as determined by experiment and theory, agree well. The theoretical predictions extend to large clusters and show nearly maximum f_s values. The CO probe quickly becomes fully solvated (see Supplemental Material [34]), and the clusters remain liquidlike as N increases, a result consistent with the enhanced f_s values shown in Fig. 2(c). Beyond $N = 10$, the superfluid fraction with respect to CO rotation is essentially 1. This means that B_{eff} will be the same as that of a free CO molecule's and that the effective inertia will be 0. This is why the two-fluid values are not shown in Figs. 2(a) and 2(b). This behavior is quite different from what was observed in clusters doped with heavier linear molecules that have much smaller rotational constants. As mentioned above, simulations of $(p\text{-}H_2)_N$-OCS clusters predict only partial decoupling of $(p\text{-}H_2)_N$ density from cluster rotation for $N \geq 14$ and associate this with an increase in the superfluid p-H_2 fraction [18]. The situation is much improved for $(p\text{-}H_2)_N$-CO_2 clusters [4], although larger clusters lose most of their superfluid response due to localization. Those f_s values are shown in Fig 2(c) to highlight the difference between the CO and CO_2 probes. The minimum at $N = 6$ for CO is due to a structural change at $N = 7$ where the hydrogen particles start to completely surround the CO dopant leading to more bosonic exchanges and therefore a greater superfluid response. For CO_2, $N = 5$ is a superfluidity minimum because the hydrogen particles are localized on a ring [4].

In summary, we measured the $J = 1 \leftarrow 0$ microwave transitions of carbon monoxide solvated with $N = 2$–8 p-H_2 molecules. We propose a novel theory for the interpretation of rotational transition frequencies in order to determine the experimental effective cluster moments of inertia and superfluid response with respect to molecule rotation. The resulting average effective moment of inertia is significantly smaller than that predicted by a classical model, thus indicating significant decoupling of hydrogen from probe rotation. With the aid of PIMC simulations, it is deduced that in contrast to $(p\text{-}H_2)_N$-CO_2 where superfluid response dies off for large N [4], the CO-doped clusters exhibit persistent and maximum superfluid response with respect to probe rotation as they grow. It will be interesting to see if larger clusters remain liquidlike in the presence of a light probe, and how their superfluid response to probe rotation will differ from the usual space-fixed frame response.

We acknowledge M. Gingras, L. Huntington, A. R. W. McKellar, R. Melko, M. Nooijen, and Tao Zeng for stimulating discussions. This research has been supported by the Natural Sciences and Engineering Research Council of Canada (NSERC) and the Canada Foundation for Innovation (CFI). We thank the Shared Hierarchical Academic Research Computing Network (SHARCNET) for computing time.

*wolfgang.jaeger@ualberta.ca
†pnroy@uwaterloo.ca

[1] V. L. Ginzburg and A. A. Sobyanin, JETP Lett. **15**, 242 (1972).
[2] K. Kuyanov-Prozument and A. F. Vilesov, Phys. Rev. Lett. **101**, 205301 (2008).
[3] S. M. Apenko, Phys. Rev. B **60**, 3052 (1999).
[4] H. Li, R. J. Le Roy, P.-N. Roy, and A. R. W. McKellar, Phys. Rev. Lett. **105**, 133401 (2010).
[5] T. E. Markland, J. A. Morrone, B. J. Berne, K. Miyazaki, E. Rabani, and D. R. Reichman, Nature Phys. **7**, 134 (2011).
[6] J. Tang, Y. Xu, A. R. W. McKellar, and W. Jäger, Science **297**, 2030 (2002).
[7] A. R. W. McKellar, Y. Xu, and W. Jäger, Phys. Rev. Lett. **97**, 183401 (2006).
[8] S. Moroni, A. Sarsa, S. Fantoni, K. E. Schmidt, and S. Baroni, Phys. Rev. Lett. **90**, 143401 (2003).

[9] F. Paesani, A. Viel, F. A. Gianturco, and K. B. Whaley, Phys. Rev. Lett. **90**, 073401 (2003).
[10] S. Grebenev, B. Sartakov, J. P. Toennies, and A. F. Vilesov, Science **289**, 1532 (2000).
[11] S. Grebenev, E. Lugovoi, B. G. Sartakov, J. P. Toennies, and A. F. Vilesov, Faraday Discuss. **118**, 19 (2001).
[12] S. Grebenev, B. G. Sartakov, J. P. Toennies, and A. F. Vilesov, Europhys. Lett. **83**, 66008 (2008).
[13] J. Tang and A. R. W. McKellar, J. Chem. Phys. **116**, 646 (2002).
[14] J. Tang and A. R. W. McKellar, J. Chem. Phys. **121**, 3087 (2004).
[15] C. Callegari, K. K. Lehmann, R. Schmied, and G. Scoles, J. Chem. Phys. **115**, 10090 (2001).
[16] F. Stienkemeier and K. K. Lehmann, J. Phys. B-At. Mol. Opt. Phys. **39**, R127 (2006).
[17] B. S. Dumesh and L. A. Surin, Phys. Usp. **49**, 1113 (2006).
[18] F. Paesani, R. E. Zillich, Y. Kwon, and K. B. Whaley, J. Chem. Phys. **122**, 181106 (2005).
[19] P. Sindzingre, D. M. Ceperley, and M. L. Klein, Phys. Rev. Lett. **67**, 1871 (1991).
[20] F. Mezzacapo and M. Boninsegni, Phys. Rev. Lett. **97**, 045301 (2006).
[21] S. A. Khairallah and D. M. Ceperley, Phys. Rev. Lett. **95**, 185301 (2005).
[22] J. E. Cuervo and P.-N. Roy, J. Chem. Phys. **125**, 124314 (2006).
[23] S. Baroni and S. Moroni, Chem. Phys. Chem. **6**, 1884 (2005).
[24] E. Knuth, S. Schaper, and J. P. Toennies, J. Chem. Phys. **120**, 235 (2004).
[25] L. A. Surin, A. V. Potapov, B. S. Dumesh, S. Schlemmer, Y. Xu, P. L. Raston, and W. Jäger, Phys. Rev. Lett. **101**, 233401 (2008).
[26] S. Moroni, M. Botti, S. De Palo, and A. R. W. McKellar, J. Chem. Phys. **122**, 094314 (2005).
[27] Y. Xu, N. Blinov, W. Jäger, and P.-N. Roy, J. Chem. Phys. **124**, 081101 (2006).
[28] H. Li, N. Blinov, P.-N. Roy, and R. J. Le Roy, J. Chem. Phys. **130**, 144305 (2009).
[29] M. Boninsegni, N. Prokof'ev, and B. Svistunov, Phys. Rev. Lett. **96**, 070601 (2006).
[30] A. V. Potapov, L. A. Surin, V. A. Panfilov, B. S. Dumesh, T. F. Giesen, S. Schlemmer, P. L. Raston, and W. Jäger, Astrophys. J. **703**, 2108 (2009).
[31] J. Tang and A. R. W. McKellar, J. Chem. Phys. **119**, 5467 (2003).
[32] R. N. Zare, *Angular Momentum: Understanding Spatial Aspects in Chemistry and Physics* (Wiley, New York, 1988).
[33] D. M. Ceperley, Rev. Mod. Phys. **67**, 279 (1995).
[34] See Supplemental Material at http://link.aps.org/supplemental/10.1103/PhysRevLett.108.253402 for a figure representing the differential hydrogen densities ($\Delta\rho_N = \rho_N - \rho_{N-1}$) in the frame of the CO molecule.